

Solvation of Calcium Ion in Polar Solvents: An X-ray Diffraction and *ab Initio* Study

Tünde Megyes, Tamás Grósz, Tamás Radnai,* Imre Bakó, and Gábor Pálinkás

Chemical Research Center, Hungarian Academy of Sciences, P.O. Box 17, Budapest H-1525, Hungary

Received: March 15, 2004

Ab initio calculations and X-ray diffraction experiments were carried out to study the structure of solutions of calcium chloride in water and methanol. *Ab initio* calculations were performed at MP2 level and density functional calculations at B3LYP level on calcium–water and calcium–methanol clusters yielding the formation of stable calcium–water clusters with up to eight water molecules and calcium–methanol clusters with up to seven methanol molecules. The experiments were performed in a wide concentration range both in water and in methanol (1–6 M and 1–2 M, respectively). The coordination number of the cation in low-concentration (1 M) aqueous and methanol solutions could only be determined with great uncertainty due to the low weights of cation–solvent contributions to the X-ray scattering intensity for both series of solutions. It was found that in 1 M solutions the Ca^{2+} ion is surrounded by eight (five to ten) water and six (four to seven) methanol molecules, respectively. The coordination numbers decrease with an increase in concentration. The accuracy of the coordination numbers determined increases with increasing concentration. The solvation shell of Cl^- ion is composed of six solvent molecules in each solution. We have found evidence of both contact and solvent-separated Ca–Cl ion pair formation at higher concentrations. On the basis of the stoichiometry of the solution and structural parameters obtained, different models are suggested to explain the liquid structure of the solutions.

1. Introduction

Structure of solvated ions in solution has long been an attractive subject for studies by means of both experimental (spectroscopic and diffraction) and theoretical (*ab initio*, molecular dynamics simulation, etc.) methods.^{1–3} Due to the key role of calcium ion in many biological reactions, there is a great interest in understanding the solvation of this important ion in detail. There are many experimental^{4–12} and theoretical^{4,12–23} reports about the hydration of calcium ion in water,^{4–23} but only a few solvation studies can be found in methanol and other alcohols.^{24–27} However, the published results still exhibit a rather diversified picture, even for such fundamental properties as the average number of coordinating solvent molecules. Structural parameters for calcium solvation in water and methanol obtained by different methods are included in Table 1.

Coordination numbers for the calcium ion in aqueous solutions obtained from calculations with simple *ab initio* pair potentials are around 9.0–9.3,^{4,18} while those resulting from calculations with potentials where many-body effects have been included are in the range 7.0–8.6.^{11,16–18}

Car–Parinello molecular dynamics simulations resulted in coordination number 6–8 for calcium.^{22–23} From X-ray diffraction experiments on calcium halide aqueous solutions, coordination numbers between 6 and 8 have been reported.^{4–11} Neutron diffraction experiments yielded a value of 10, a rather unexpectedly high value, for a less concentrated solution (around 1 M) and a value between 5.5 and 6.4 for more concentrated solutions (4–5 M).^{8,9} Recent extended X-ray absorption fine structure (EXAFS) measurements resulted in coordination number of calcium ion between 7 and 8.^{10,12}

Cluster calculations by density functional theory (DFT) have shown that for isolated clusters of $\text{Ca}(\text{H}_2\text{O})_n^{2+}$ with $n = 1–8$

the highest stability is reached at $n = 6$.¹⁹ However, the DFT calculations represent gas-phase conditions at 0 K temperature limit. In real solutions and at ambient temperature, the space requirement of the molecules and the interactions between them are completely different from the DFT case; consequently, the coordination number can reach an even higher value than six.

There are only a few studies published on the solvation of calcium ion in methanol; for example, the total solvation number of calcium chloride has been reported in methanol media,²⁶ a Monte Carlo simulation was performed of calcium ion in several solvents including methanol,²⁷ and dynamics of solvation^{24,25} has also been studied. Nevertheless, no systematic structural study has been reported on the liquid structure of concentrated calcium–halide–methanol ternary systems.

A special point of interest for concentrated solutions is the structure of solvates at high concentration range. Indeed, in methanol, if concentration of CaX_2 salts (X is chloride, iodide, or bromide) increases above $2 \text{ mol} \cdot \text{dm}^{-3}$, the stoichiometry of the solutions will not allow the formation of independent solvate shells neither for cations nor for anions any more, and solvent-separated and even contact ion pairs are expected to be formed in abundance in solution. There is a number of various possible structural forms displaying drastic changes both in the cationic solvates and in the bulk of the solution in comparison with the dilute solutions. To extract the possible structural forms in such a liquid, extensive model building and testing is necessary. Computer simulation studies can help us to resolve the microscopic structures as well. In addition, the high concentration range might give a good chance to observe some “clusters” in solution, and their composition can be directly compared to clusters observed by other methods, for example, mass spectrometry.

To understand this uncertainty in the coordination number of calcium, it is worth considering that each study suffers from certain limitations, which might be responsible for this in-

* To whom correspondence should be addressed. E-mail: radnait@chemres.hu. Tel: (+36)(1) 4384141/ext. 114. Fax: (+36)(1) 3257554.

TABLE 1: Comparison of the Structural Parameters of the Solvation Shell of Calcium Obtained from Different Studies

solvent	salt	<i>c</i> (mol dm ⁻³)	method ^b	<i>r</i> (Å)	<i>n</i>	ref
water	CaCl ₂	1.1	XD	2.39	6.9	4
	CaCl ₂	3.3	XD	2.40	8	5
	CaCl ₂	5.2	XD	2.40	8	5
	Ca(NO ₃) ₂	3.6	XD	2.44	7	6
	Ca(NO ₃) ₂	6	XD	2.45	7	6
	CaCl ₂	1	XD	2.42	6	7
	CaCl ₂	2	XD	2.41	6	7
	CaCl ₂	4.5	XD	2.42	6	7
	CaCl ₂	2	XD	2.46	8	11
	CaBr ₂	1.5	XD	2.46	8	11
	CaBr ₂	1.5	XD	2.46	8	11
	CaI ₂	1.5	XD	2.46	8	11
	CaCl ₂	1	ND	2.46	10	9
	CaCl ₂	2.8	ND	2.39	7.2	9
	CaCl ₂	4.5	ND	2.40	6.4	9
	CaCl ₂	4.5	ND	2.41	5.5	8
	CaCl ₂	0.12	EXAFS	2.46	8.0	10
	CaCl ₂	0.2	EXAFS	2.43	6.8	12
	CaCl ₂	6.0	EXAFS	2.44	7.2	12
	Ca ²⁺		PCM MD	2.5	8.6	14
	Ca ²⁺		cMD	2.49	9–10	13
	Ca ²⁺		cMD	2.5	8	17
	Ca ²⁺		cMD	2.5	7.9	16
	CaCl ₂		cMD	2.39	9.2	4
	Ca ²⁺		cMD1	2.40	8	11
	Ca ²⁺		cMD2	2.46	8	11
	Ca ²⁺		cMD3	2.51	9–10	11
Ca ²⁺		cMD	2.47	9.2	18	
Ca ²⁺		QM/MM	2.38	10	18	
Ca ²⁺		QM/MM	2.46–2.51	7.1–8.1	20	
Ca ²⁺		C–P	2.42	6	22	
Ca ²⁺		C–P	2.64	7–8	23	
Ca ²⁺		MC	2.4	7.01	15	
methanol	CaCl ₂	5.66 ^a	visc		5.5	26
	Ca ²⁺		MC	2.3	7	27

^a In mol kg⁻¹. ^b Abbreviations: XD, X-ray diffraction; ND, neutron diffraction; EXAFS, extended X-ray absorption fine structure; PCM MD, polarizable continuum model molecular dynamics; cMD, classical molecular dynamics; QM/MM, quantum mechanics/molecular mechanics; C–P, Car–Parinello; MC, Monte Carlo; visc, viscosity study.

homogeneous picture concerning the hydration of calcium. It would be inevitable for all studies to make clear statements on limitations and uncertainties inherent to the methods applied.

Based on these considerations, in the present paper a concentration series of systematic X-ray diffraction studies is reported on CaCl₂ solutions both in water and methanol, together with density functional calculations at B3LYP²⁸ and MP2 levels for calcium–water and calcium–methanol systems. Special attention will be devoted to the reliability of the conclusions drawn based on either theory or analysis of experimental data.

2. Ab Initio Study

In a recent work,²² density functional studies and Car–Parinello (CP) molecular dynamics simulations of small [Ca(H₂O)_{*n*}]²⁺ clusters with *n* = 1–9 water molecules, together with Car–Parrinello simulation of the Ca²⁺ ion in a periodic box of 54 water molecules, have been performed using the BLYP functional, that is, the exchange functional given by Becke and the correlation energy expression by Lee, Yang, and Parr.²⁸ It was found that stable highly symmetric calcium–water clusters can be formed with up to eight water molecules and the *n* = 9 cluster dissociates into the last stable [Ca(H₂O)₈]²⁺ complex. In the CP simulation of Ca²⁺ ion with 54 water molecules, the Ca²⁺ ion resulted to be coordinated by six water molecules in an octahedral arrangement.

To study structure and energy of [Ca(H₂O)_{*n*}]²⁺ and [Ca(CH₃OH)_{*n*}]²⁺ clusters with *n* = 1–9 water and methanol molecules, DFT calculations with the B3LYP²⁸ method have been carried out. This method is based on empirically parametrized hybrid functional including Hartree–Fock exchange and gradient corrections of the density. The B3LYP functional has already been proven to result in more accurate energy of hydrogen-bonded systems than results achieved by BLYP functional. Simultaneously, MP2 level calculations were also performed to check accuracy of DFT calculations carried out with B3LYP functional. All of the calculations were performed using Gaussian 98.²⁹ The basis set applied for all optimization and frequency calculations was the 6-311+G** set. It was already shown that using this basis set one can describe the Ca²⁺–H₂O interaction quite well.^{22,30} The B3LYP DFT calculations give reasonable agreement with spectroscopy data and are only slightly lower in accuracy than results of ab initio MP2.

The structures of each complex (Ca²⁺(H₂O)_{*n*}, Ca²⁺(CH₃OH)_{*n*}) were fully optimized by searching for a minimum in their potential hyper surface. Taking into account the fact that the potential surfaces for this type of cluster are flat, the TIGHT convergence criterion was used in the Gaussian 98 program package. At each stationary point of the B3LYP calculations thus located, a vibrational study was performed to confirm that the given point was a minimum on the potential surface. No symmetry restrictions were imposed during the optimization.

The interaction energy at each minimum configuration was calculated by the supermolecule method. All interaction energies were corrected for the basis set superposition error (BSSE) by using the counterpoise method.³¹ The BSSE correction was about 2–4% of total interaction energy.

In agreement with recent DFT calculations with BLYP functional, the calcium ion was found to form stable hydrates up to eight water molecules. The insertion of the ninth water molecule into the hydration shell was practically not possible. In Table 2, interaction energies, the intramolecular OH distance, and the HOH angle, as well as the Ca–O distance, for the clusters studied are given.

In the lowest energy gas-phase structure of the Ca(H₂O)₆²⁺ cluster, water molecules coordinate the calcium ion symmetrically by an antipole orientation. The distance between water molecules in different clusters with *n* > 6 gradually decreases with *r*_{OO} = 3.42, 3.05, and 2.93 Å for *n* = 6, 7, and 8, respectively. Figure 1 shows the binding energy of water molecules,

$$\Delta E_{\text{tot}}/n = \{E(\text{Ca}(\text{H}_2\text{O})_n^{2+}) - E(\text{Ca}^{2+}) - nE(\text{H}_2\text{O})\}/n \quad (1)$$

together with the energy required to remove one water molecule from a given cluster,

$$|\Delta E_{\text{inc}}| = |E(\text{Ca}(\text{H}_2\text{O})_n^{2+}) - E(\text{Ca}(\text{H}_2\text{O})_{n-1}^{2+}) - E(\text{H}_2\text{O})| \quad (2)$$

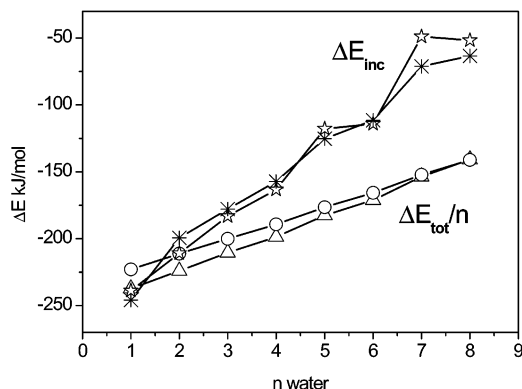
The binding energy of water shows a linearly decreasing trend as more water molecules are added to the hydration shell. It is worth noting, however, that the energy required to remove one water molecule from clusters as a function of the number of hydrate molecules, $|\Delta E_{\text{inc}}|$, shows two plateaus at *n* = 5, 6 and 7, 8 water molecules with an energy difference of about 50 kJ mol⁻¹. The energy required to remove one water molecule from a cluster with *n* = 8 water molecules, $|\Delta E_{\text{inc}}| \approx 50$ –55 kJ mol⁻¹ is not much larger than the typical energy of a strong hydrogen bond between two water molecules. Similar results were found in the recent DFT calculation using BLYP functional.²² These

TABLE 2: Interaction Energies, $\Delta E = E(\text{Ca}(\text{H}_2\text{O})_n^{2+}) - E(\text{Ca}^{2+}) - nE(\text{H}_2\text{O})$ (kJ mol⁻¹), the Intramolecular OH Distance, $r_{\text{O-H}}$, in Å, COH Angle, ϑ_{HOH} , in deg, and the Ca-O Distance, $r_{\text{Ca-O}}$, in Å Obtained by DFT Calculations at B3LYP and MP2 Levels for $\text{Ca}(\text{H}_2\text{O})_n^{2+}$ Clusters

clusters	$-\Delta E$		$r_{\text{O-H}}$		$r_{\text{Ca-O}}$		ϑ_{HOH}	
	B3LYP	MP2	B3LYP	MP2	B3LYP	MP2	B3LYP	MP2
$\text{Ca}(\text{H}_2\text{O})^{2+}$	237.22	222.96	0.976	0.972	2.243	2.276	104.24	103.06
$\text{Ca}(\text{H}_2\text{O})_2^{2+}$	448.10	422.31	0.974	0.970	2.282	2.308	104.28	103.06
$\text{Ca}(\text{H}_2\text{O})_3^{2+}$	631.26	600.12	0.972	0.969	2.313	2.330	104.55	103.30
$\text{Ca}(\text{H}_2\text{O})_4^{2+}$	794.58	757.29	0.970	0.967	2.342	2.351	104.74	103.51
$\text{Ca}(\text{H}_2\text{O})_5^{2+}$	912.29	882.52	0.969	0.966	2.360	2.370	104.94	103.78
$\text{Ca}(\text{H}_2\text{O})_6^{2+}$	1026.44	993.92	0.967	0.965	2.401	2.401	105.37	104.19
$\text{Ca}(\text{H}_2\text{O})_7^{2+}$	1075.31	1065.06	0.966	0.964	2.450	2.455	105.89	104.30
$\text{Ca}(\text{H}_2\text{O})_8^{2+}$	1126.93	1128.35	0.966	0.963	2.482	2.482	106.16	104.76

TABLE 3: Interaction Energies, ΔE (kcal mol⁻¹), the Intramolecular OH Distance, $r_{\text{O-H}}$ (Å), COH Angle, ϑ_{COH} (deg), and the Ca-O Distance, $r_{\text{Ca-O}}$ (Å), Obtained at B3LYP and MP2 Levels in $\text{Ca}(\text{CH}_3\text{OH})_n^{2+}$ Clusters

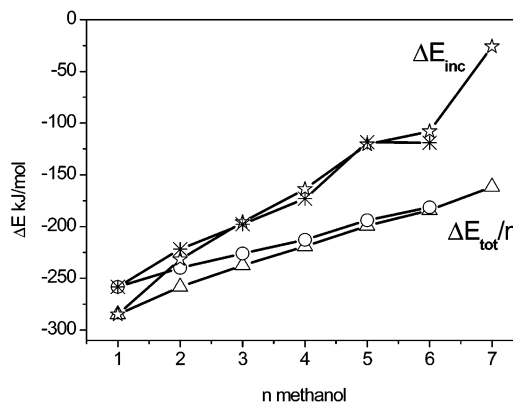
clusters	$-\Delta E$		$r_{\text{O-H}}$		$r_{\text{Ca-O}}$		ϑ_{HOH}	
	B3LYP	MP2	B3LYP	MP2	B3LYP	MP2	B3LYP	MP2
$\text{Ca}(\text{CH}_3\text{OH})^{2+}$	285.03	258.24	0.973	0.970	2.19	2.23	106.79	106.77
$\text{Ca}(\text{CH}_3\text{OH})_2^{2+}$	516.69	480.07	0.969	0.968	2.24	2.27	106.90	106.51
$\text{Ca}(\text{CH}_3\text{OH})_3^{2+}$	712.48	677.79	0.968	0.967	2.28	2.30	107.30	106.26
$\text{Ca}(\text{CH}_3\text{OH})_4^{2+}$	876.29	850.78	0.967	0.965	2.32	2.33	107.60	106.82
$\text{Ca}(\text{CH}_3\text{OH})_5^{2+}$	996.89	969.23	0.966	0.965	2.37	2.37	107.90	107.12
$\text{Ca}(\text{CH}_3\text{OH})_6^{2+}$	1104.82	1098.3	0.965	0.965	2.40	2.38	108.32	107.90
$\text{Ca}(\text{CH}_3\text{OH})_7^{2+}$	1130.77				2.42	2.84		

**Figure 1.** Binding energies, $\Delta E_{\text{tot}}/n$ and ΔE_{inc} , in kJ mol⁻¹ in $[\text{Ca}(\text{H}_2\text{O})_n^{2+}]$ clusters for $n = 1-8$ obtained by density functional theory (Δ, \star) and MP2 ($\circ, *$) calculations.

results indicate that besides the most stable octahedral complex, calcium-water clusters with $n = 7$ and 8 water molecules may also coexist in the liquid phase and they are substantially influenced by outer neighbors.

The geometrical parameters for the $\text{Ca}^{2+}(\text{H}_2\text{O})_n$ clusters are in agreement with those reported elsewhere.^{19,21,22,32} In our calculations, a more flexible basis set was used than those in earlier calculations, and we take into account the electron correlation at MP2 level as well. In these clusters, the oxygen atoms face the cation forming thus a so-called “interior structure”. The geometry of water ligand changes only slightly with increase of the hydration number. The OH bond becomes longer by about 0.01 Å, and the HOH bond angles increase by about 1.5°. The Ca-O bond length increases steadily with increasing number of water molecules in the first shell.

Both levels of theory are in good agreement, within 1% difference, in the obtained geometric parameters of $\text{Ca}(\text{H}_2\text{O})_n^{2+}$ clusters. For all $\text{Ca}(\text{H}_2\text{O})_n^{2+}$ clusters, the B3LYP method overestimates the interaction energies as compared to the calculation at MP2 level. The OH frequencies have a red shift, which decreases with increasing number of water molecules in the first shell. The bending frequencies have a blue shift. The experimental OH frequency shift³³ of the water molecule in the first shell of calcium is about 50 cm⁻¹.

**Figure 2.** Binding energies, $\Delta E_{\text{tot}}/n$ and ΔE_{inc} , in kJ mol⁻¹ in $[\text{Ca}(\text{CH}_3\text{OH})_n^{2+}]$ clusters for $n = 1-6$ obtained with density functional theory (Δ, \star) and MP2 ($\circ, *$) calculations.

The geometrical parameters for the $\text{Ca}^{2+}(\text{CH}_3\text{OH})_n$ clusters are presented in Table 3. Structures with more than seven methanol molecules in the primary shell could not be observed.

The molecular symmetries of the clusters for $n = 1-6$ are very close to the corresponding theoretical geometrical symmetries of the given clusters. The arrangement of O atoms around the cation is the same as that found in the calcium-water clusters. The Ca-O distances increase with increasing number of ligands added to the complexes due to the repulsion between the ligands. The cluster with seven methanol molecules is somewhat special: it produces a distorted geometry. Six water molecules are located around the cation at 2.42 Å, while the seventh one is elongated at 2.8 Å.

Figure 2 shows the binding energy of methanol molecules, $\Delta E_{\text{tot}}/n$, together with the energy, ΔE_{inc} , required to remove one methanol molecule from a given cluster. The behavior of these energies as a function of the number of solvated molecules resembles those of aqueous clusters. The plateau in ΔE_{inc} appears at $n = 6$ methanol molecules and removal of a molecule from the cluster with $n = 7$ requires much less energy, ~ 26 kJ mol⁻¹, than that for $n = 6$ cluster.

Similar to the aqueous solution of calcium, the OH frequencies have a red shift, which decreases with increasing number

of methanol molecules in the first shell; the bending COH frequencies have a blue shift.

As it was experienced for the hydration case, the overall results provided by both the DFT and MP2 methods are very similar; but in all cases, the B3LYP method overestimates the Ca–O distance, as well as the interaction energy. The interaction energy is about 10–15% greater in the $\text{Ca}^{2+}(\text{CH}_3\text{OH})_n$ complexes than in the $\text{Ca}^{2+}(\text{H}_2\text{O})_n$ complexes. This is not too much compared to the available literature result. A theoretical study of complexes formed by methanol for Li^+ and Na^+ ions have already been performed in the same calculation levels.³⁴ The interaction energy of these clusters is about 30–50% smaller than that in the calcium–methanol complexes.

Ca–Cl ion pairs in aqueous and methanol media were also studied using B3LYP method in the following compositions: $[\text{CaCl}(\text{H}_2\text{O})_7]$ (I), $[\text{CaCl}(\text{H}_2\text{O})_5]$ (II), $[\text{CaCl}_2(\text{H}_2\text{O})_4]$ (III), and $[\text{CaCl}(\text{CH}_3\text{OH})_5]$ (IV). Geometrical parameters for the complexes are as follows: (I) $r_{\text{Ca-Cl}} = 2.85$, $r_{\text{Ca-O}} = 2.46$, (II) $r_{\text{Ca-Cl}} = 2.70$, $r_{\text{Ca-O}} = 2.43$, (III) $r_{\text{Ca-Cl}} = 2.72$, $r_{\text{Ca-O}} = 2.42$, and (IV) $r_{\text{Ca-Cl}} = 2.65$, $r_{\text{Ca-O}} = 2.40$ Å. Similar structures were found in the crystal state.³⁵ Such ion pairs could appear in highly concentrated solutions when the number of solvent molecules present is not enough to fully solvate the ions.

3. X-ray Scattering Measurements

3.1. Experimental Details. All solutions were prepared from distilled water and methanol of high purity (anhydrous, special grade, Merck) and from anhydrous CaCl_2 (anhydrous, 99.99%, Aldrich). No further purification was performed. X-ray measurements were carried out on solutions of calcium chloride in water and methanol (Table 4) at various concentrations.

The X-ray scattering measurements were made at ambient temperature (24 ± 1 °C), on a Θ – Θ goniometer with symmetrical transmission geometry and by using Mo $K\alpha$ radiation ($\lambda = 0.7107$ Å wavelength) with a graphite monochromator placed in the diffracted beam. The liquid sample holder had plane-parallel windows prepared from 6.3 μm thick Mylar foils. The scattering angle range of measurement spanned over $1.28^\circ \leq 2\Theta \leq 120^\circ$ corresponding to a range of $0.2 \leq k \leq 15.3$ Å⁻¹ of the scattering variable $k = (4\pi/\lambda)\sin \Theta$. Over 100 000 counts were collected at each of 150 discrete angles selected in $\Delta k \approx 0.1$ Å⁻¹ steps in several repeated runs (20 000 counts at each point).

The measurement technique and data treatment were essentially the same as described previously.³⁶

The measured intensities were corrected for background, polarization, absorption, and Compton scattering.³⁷ The Compton contribution was evaluated by a semiempirical method to account for the monochromator discrimination.³⁸ The Compton intensities needed for the corrections were calculated with analytical formulas.^{39,40} The experimental structure function is defined as

$$h(k) = \frac{I(k) - \sum_{\alpha} x_{\alpha} f_{\alpha}^2(k)}{M(k)} \quad (3)$$

where $I(k)$ is the corrected coherent intensity of the scattered beam normalized to electron units,⁴¹ $f_{\alpha}(k)$ and x_{α} are the scattering amplitude and mole fraction for a type of α particle, respectively, and $M(k)$ is the modification function, $M(k) = [\sum x_{\alpha} f_{\alpha}(k)]^2 \exp(0.01k^2)$. The coherent scattering amplitudes of the ions and the methanol molecule were computed according to analytical formulas suggested by Hajdu³⁹ and Cromer et al.⁴²

TABLE 4: Physical Properties of CaCl_2 Solutions Studied^a

solvent	c (mol dm ⁻³)	ρ (g cm ⁻³)	μ (cm ⁻¹)	ρ_0 (cm ⁻²⁴)
water	1	1.07	2.61	0.0980
	2.5	1.19	4.94	0.0961
	4	1.31	7.27	0.0942
	6	1.36	10.26	0.0807
methanol	1	0.89	2.07	0.0899
	2	1.98	3.49	0.0895

^a Symbols: c , salt concentration; ρ , mass density; μ , linear X-ray absorption coefficient; ρ_0 , atomic number density.

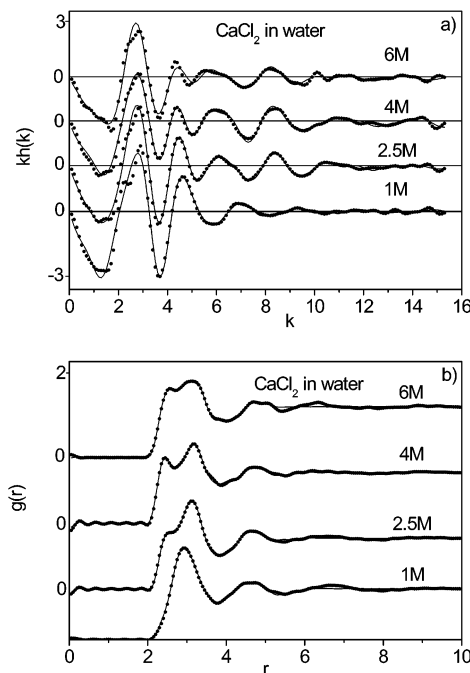


Figure 3. Structure functions, $h(k)$, multiplied by k (a) and pair correlation functions, $g(r)$ (b), for calcium chloride solutions in water. The experimental values are given by dotted lines and the theoretical values by solid lines.

The water and methanol molecules were treated in atomic representation. The necessary parameters were taken from International Tables for X-ray Crystallography.⁴³

The experimental pair correlation function was computed from structure function $h(k)$ by Fourier transformation according to

$$g(r) = 1 + \frac{1}{2\pi^2 r \rho_0} \int_{k_{\min}}^{k_{\max}} kh(k) \frac{\sin(kr) dk}{M(k)} \quad (4)$$

where r is the interatomic distance, k_{\min} and k_{\max} are the lower and upper limits of the experimental data, and ρ_0 is the bulk number density of the stoichiometric units. After repeated Fourier transformations when the nonphysical peaks present in the $g(r)$ at small r values were removed, the structure function was corrected for residual systematic errors.⁴⁴ In this process, the peak due to the intramolecular C–O distance centered at about 1.45 Å was also removed.

An alternative form of radial distribution function is usually given as $D(r) - 4\pi r^2 \rho_0$, and it is calculated from $g(r)$ functions with $D(r) = 4\pi r^2 \rho_0 g(r)$.

3.2. Method of Structural Analysis. The observed structure functions $kh(k)$ and radial distribution functions $g(r)$ as obtained for a set of solutions in water and methanol are shown in Figures 3 and 5, respectively. As a first step, the visual evaluation and a preliminary semiquantitative analysis was performed, when

TABLE 5: Structural Parameters for the Aqueous Solution of CaCl₂ with the Estimated Errors in the Last Digits^a

sample	bond type	<i>r</i>	σ	<i>n</i>
1 M	Ca–O	2.46(1)	0.20	8.0
	Ca–O ^{II}	4.55(2)	0.23	13.0(5)
	Cl–O	3.25(1)	0.19	6.0(3)
	O ^I –O ^I	4.75(2)	0.23	2.0
	O–O	2.85(1)	0.20	4.3(1)
2.5 M	Ca–O	2.43(1)	0.19	6.9(3)
	Ca–O ^{II}	4.55(3)	0.23	11.1(7)
	Cl–O	3.25(1)	0.19	6.2(1)
	O ^I –O ^I	4.75(2)	0.23	1.5
	O–O	2.99(1)	0.20	4.0
4 M	Ca–O	2.43(2)	0.15	5.8(3)
	Ca–O ^{II}	4.55	0.23	7.2
	Ca–Cl	2.74(2)	0.17	1.0(2)
	Ca–Cl ^{III}	4.86(2)	0.23	2.1(2)
	Cl–O	3.25(1)	0.20	4.5(3)
	Cl–O ^I	3.79(3)	0.20	2.0
	O–O	2.99(1)	0.20	3.7(1)
	O–O	2.45(1)	0.17	5.1(3)
6 M	Ca–O ^{II}	4.55	0.23	5.0
	Ca–Cl	2.72(2)	0.17	1.5
	Ca–Cl ^{III}	4.85(2)	0.23	3.0(2)
	Cl–O	3.24(1)	0.20	4.1(3)
	Cl–O ^I	3.80(3)	0.21	3.0
	O–O	2.95(1)	0.20	3.7(1)
	O–O	2.95(1)	0.20	3.7(1)

^a The distances (*r*) and the mean square deviations (σ) are given in Å.

the radial distribution functions for all solutions were compared with those available in the literature. Further on, the observed data were analyzed by geometrical model constructions and fitting the model structure functions to the corresponding experimental ones by nonlinear least-squares method (LSQ). The quality of fit was monitored through the S_{res} factor as defined by

$$S_{\text{res}} = \sum_{k_{\text{min}}}^{k_{\text{max}}} k^2 [h_{\text{expt}}(k) - h_{\text{calcd}}(k)]^2 \quad (5)$$

The theoretical intensities, $h_{\text{calcd}}(k)$ were calculated by formulas

$$h_{\text{calcd}}(k) = h_{\text{d}}(k) - h_{\text{c}}(k) \quad (6)$$

$$h_{\text{d}}(k) = \sum_{\alpha\beta} \frac{x_{\alpha} n_{\alpha\beta} f_{\alpha} f_{\beta} \sin(kr_{\alpha\beta})}{M(k) kr_{\alpha\beta}} \exp\left(-\frac{\sigma_{\alpha\beta}^2 k^2}{2}\right) \quad (7)$$

$h_{\text{c}} =$

$$\sum_{\alpha\beta} 4\pi\rho_0 \frac{x_{\alpha} x_{\beta} f_{\alpha} f_{\beta} k R_{\alpha\beta} \cos(kR_{\alpha\beta}) - \sin(kR_{\alpha\beta})}{M(k) k^3} \exp\left(\frac{\Gamma_{\alpha\beta}^2 k^2}{2}\right) \quad (8)$$

where α and β refer to scattering centers of different chemical types. The first term, $h_{\text{d}}(k)$ (discrete part), is related to the short-range interactions characterized by the interatomic distance $r_{\alpha\beta}$, the root-mean-square deviation $\sigma_{\alpha\beta}$, and the coordination number $n_{\alpha\beta}$. The second term, $h_{\text{c}}(k)$ (continuum part), accounts for the uniform distribution of β -type particles around α -type particles beyond a given distance; $R_{\alpha\beta}$ and $\Gamma_{\alpha\beta}$ define the related boundary of the uniform distribution of α, β -type distances and their root-mean-square deviation, respectively. Consequently, one contribution for each type of interaction was involved in $h_{\text{d}}(k)$ and $h_{\text{c}}(k)$ functions (eqs 7 and 8), as shown in Table 5.

An inspection of the radial distribution functions indicated to us that they are rather composite and no peaks, not even the main peak can be uniquely assigned to a certain kind of

interaction. In the case of aqueous solutions, for example, the first peak is centered around 2.9 Å in 1 M solution and splits into two peaks at higher concentrations, showing that more than one interaction gives rise to this peak. To give a quantitative description of the structure, that is, to derive the structural parameters, the coordination numbers, mean interatomic distances, and their root-mean-square deviations, at least for the contributions of the predominant interactions, the construction and fitting of extensive structural models were performed.

The fitting strategy was the following. At the beginning, the “rough” structure of ionic shells has been fixed by inputting the structural parameters obtained from the preliminary study of radial distribution functions and from the previous studies of CaCl₂ solutions in water and methanol. The parameters of the discrete structure were kept constant, and those for continuum were adjusted. The refinement extended over the *k* range $0.2 \leq k \leq 15.3 \text{ \AA}^{-1}$. In the next step, all coordination numbers were kept constant and distances and root-mean-square deviations have been adjusted. Next, most of the coordination numbers were allowed to vary. This process was repeated alternately several times until the minimum S_{res} factor has been reached. Finally an overall check was run, letting all parameters vary, covering the entire *k* range. As it can be seen, the data evaluation procedure did not comprise any geometrical constraint between the distance parameters as a consequence of any assumed regular symmetry. The models suggested were built on the basis of parameters obtained from the fitting procedure.

3.3. Results and Discussion. *3.3.1. Aqueous Solutions of CaCl₂.* For aqueous solutions of CaCl₂, the ratio of salt to the number of water molecules varies as 1:53.3, 1:20.33, 1:12.08, and 1:6.48 (see Table 5). This means that in the less concentrated (1 M) solution there are enough solvate molecules available to form complete solvation shells both for Ca²⁺ and Cl⁻ ions, assuming that the calcium ion is eight-coordinated and the chloride ion is six-coordinated and no contact ion pair is formed. This is, however, not true for the 4 M and obviously not for the most concentrated (6 M) solution, simply because of the stoichiometric conditions. The 2.5 M solution is the border case. Based on these considerations of stoichiometric composition and taking into account that whenever it is possible, the solvent molecules tend to solvate the ions at the maximum available coordination number in average, a simple 4-step model can be applied as found in the literature:⁴⁵ (1) In dilute solutions, all ions are fully solvated with at least one layer of solvate molecules; the maximum number of symmetry elements are found in the solvate shells (when symmetry considerations are applicable at all). (2) With increasing concentration, the solvated ions are still separated, but the solvate shells might become incomplete; symmetry becomes gradually distorted. (3) If the available solvent molecules further decrease in number (below the sum of the average coordination number of cations and anions), solvent-separated ion pairs occur. The original symmetry of solvate shells is distorted but may or may not change in average sense. (4) With further increase of ion concentration, the relative lack of solvent molecules will force the formation of contact ion pairs. The structures of these solvation shells can strongly differ from the original solvate structures.

It is difficult to determine quantitative conditions for when the four steps occur in general terms; however, one can decide which of the four steps is applicable from the stoichiometric composition of a given solution and from the assumptions for the probable geometry of the solvate shells. It is worth noting that according to our assumption, the governing process in ionic solution is the solvation of ions with a tendency to reach the

maximum available symmetry. Any deviation from this (e.g., concentration-dependent change in symmetry, strong tendency to form ion pairs in the liquid, etc.) can cause deviations in the expected structural forms. From the experimental point of view, two interesting questions arise: first, whether the above model can be verified by experiment, that is, can we detect the solvated ions, solvent-separated ions, or contact ion pairs as forecasted, and second, are some structural changes observable related to deviations from the simple stoichiometry-related considerations for the structure?

To be specific, for the studied systems, an interesting question is whether any Ca–Cl contact ion pairs can be detected at the 2.5 M concentration.

3.3.2. X-ray Structure Functions and Radial Distribution Functions for CaCl_2 in Water. Visible concentration variations can easily be observed when looking at the structure functions in Figure 3a, derived from the X-ray diffraction experiments. The first double peak—as it is well-known from the experience with scattering patterns of hydrogen-bonded liquids—is certainly predominated by the scattering contributions of bulk solvent of solutions. This is observable in the pure solvents' structure functions as well (not shown here).^{46,47} This “double peak feature” is gradually disappearing as the quantity of bulk solvent is reduced by concentration.

The $g(r)$ functions are shown in Figure 3b. They witness about the trivial concentration dependence of the magnitude of various contributions and of some structural changes as well. From the rather complex and broad main peak of 1 M solution in the range 2–4 Å, a steep, asymmetric first peak arises at about 2.45 Å, followed by another peak at 3.2 Å for the more concentrated solutions. The first, separate peak around 2.45 Å can be assigned to the Ca–O first-neighbor distances. By the increase of concentration, the peak increases due to the increased weight of Ca–O-type contributions to the scattering pattern. Another broad peak can be observed in the range 4–5.5 Å. This peak is difficult to resolve, and therefore an extended model analysis can only reveal the major contributions to it. It is, however, expected that the changes are not simply due to the changes in the weights of contributions to the scattering pattern but also reflect some drastic structural changes in local structure.

A better but still phenomenological analysis can be given by constructing the difference radial distribution functions, $D(r) - 4\pi r^2 \rho_0$, where the functions for less concentrated solutions are subtracted from the more concentrated ones with appropriate weighting factors accounting for the different number densities.

Figure 4a shows the difference functions after subtraction of the corresponding distributions for pure water (not shown in this paper),^{46,47} and Figure 4b shows similar functions after subtraction of radial distributions for 1 M solution. Some characteristic distances of the most important contributions based on ionic radii (Ca^{2+} 1.05, Cl^- 1.81, OH^- 1.35 Å)⁴⁸ are located and denoted in the figures as legends. In Figure 4a, a peak is observable around 2.45 Å, which can be assigned to Ca–O interaction. The Cl–O interaction is mostly responsible for the peak at 3.25 Å. The peak at 4.6 Å is rather complex: interactions belonging to the second hydration shell of the calcium ion can give rise to this peak, but also $\text{O}^{\text{I}}-\text{O}^{\text{I}}$ interactions between the oxygen atoms in the hydration shell of calcium or chloride ions and the second neighbor water–water interaction or both can contribute. This peak disappears with increasing concentration, suggesting that mostly Ca– O^{II} second hydration shell interaction is responsible for it. As it was mentioned above, with increasing concentration the solvate shells might become incomplete or destroyed. Around 4.7 and 6.3 Å, further blurred peaks can be

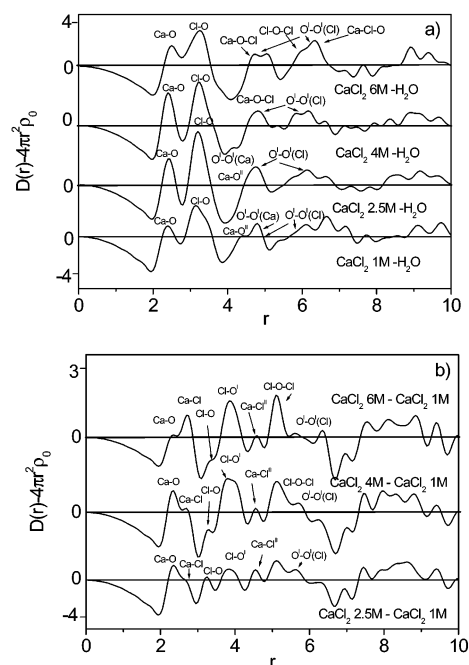


Figure 4. Difference radial distribution functions in the $D(r) - 4\pi r^2 \rho_0$ for each calcium chloride solution and pure water (a) and each calcium chloride solution and 1 M calcium chloride solution in water (b). The expected main contributions to the pair interactions are indicated by legends.

observed, but it is very difficult to give a reasonable explanation for peaks at such long distances. The oxygen–oxygen interaction between the oxygen atoms in the hydration shell of calcium and chloride ions can be responsible for the peak around 4.7 Å, but especially in high-concentration solutions, Ca– Cl^{II} solvent-separated ion pairs can contribute as well. There are very few studies in the literature^{12,49} about ion pair formation. In a previous study of highly concentrated calcium(II) chloride solutions and hydrate melts,⁴⁹ the authors supposed the presence of solvent-separated ion pairs around the distance 4.7–4.8 Å, when a chloride ion penetrates in the second hydration shell of the calcium ion. In a recently performed EXAFS experiment Fulton et al.¹² found that solvent-separated ion pairs but no contact ion pairs are formed in highly concentrated solution. Many interactions could be responsible for the peak around 6 Å. Interactions such as Ca–Cl–O, Cl–O–Cl, Ca–O–Cl (Ca– Cl^{II}), and Cl–Cl can be identified by distance estimations based on ionic radii, but oxygen–oxygen interactions in the hydration shell of chloride ion can also contribute.

In Figure 4b, some new peaks appear besides the interactions described above. At 2.7–2.8 Å, an increasing peak can be observed, which can be attributed to Ca–Cl contact ion pair. This peak increases with increasing concentration; this change can be explained by the parallel effects of the increase of the weight of Ca–Cl-type contributions and the more pronounced formation of the contact ion pairs in more highly concentrated solutions. In high-concentration solutions, the lack of solvent molecules will force the formation of different contact or solvent-separated ion pairs or both, which may be solvated by a certain number of solvent molecules. Consequently, when in the hydration shell of calcium ion one water molecule is changed to chloride ion, forming a Ca–Cl contact ion pair, around 3.8 Å $\text{Cl}^{\text{I}}-\text{O}^{\text{I}}$ interactions can appear.

Interpretation of the Structural Parameters and Model Building. The structural parameters obtained from the least-squares fit of the structure functions $h(k)$ shown in Figure 3a for the aqueous solution of CaCl_2 are given in Table 5.

An average geometrical picture of cation solvation can be derived from the obtained set of model parameters. In 1 M solution, eight water molecules surround each Ca^{2+} ion turning with their oxygen atoms toward the cation. With the increase in concentration the overall number of water molecules decreases and will be not enough to form solvation shells containing eight water molecules around Ca^{2+} ion. Consequently, the Ca–O coordination number decreases. In 1 M solution, the Ca–O^{II} second sphere is observed around 4.55 Å, containing 13 water molecules. The number of water molecules in the second sphere decreases with increase in concentration. Probably with increase in concentration, the second hydration shell of the calcium ion is destroyed and other (solvent-separated) ion–ion interactions appear instead, for example, chloride atoms penetrate in the second hydration shell.

In low-concentration solution, the Cl^- ion is solvated by six water molecules as seen from Cl–O parameters. The Cl–O coordination number decreases with increase in concentration.

The O–O interaction appears at 2.85 Å in 1 M solution, but this distance becomes longer (2.99 Å) at higher concentrations. The reason for this change is probably that the O–O interaction between water molecules in the bulk gradually decreases at higher concentrations, and instead, O–ion–O-type interactions give contributions to the radial distributions, indicating the occurrence of ion pairs. Another oxygen–oxygen interaction (O^I–O^I) was taken into account around 4.75 Å, which appears due to the interaction between the oxygen atoms involved in the hydration shell of the calcium ion.

To check whether solvent-separated or contact ion pairs are present in 2.5 M solution, we have tried to fit the structure function of the 2.5 M solution with an alternative model as well, in which preliminary assumption for the presence of ion pairs in the solution was taken. The fit happened to become slightly better by including the Ca–Cl solvent-separated and contact ion pairs as well, but we think this is not enough reason to decide whether ion pairs are present in solution (see Figure 8).

In concentrated solutions, up to 4 M, around 4.85 Å solvent-separated ion pairs (Ca–Cl^{II}) can be identified. When the concentration of solution increases the number of solvent molecules able to form the hydration shell of ions decreases so, as it was discussed above, chloride ions can enter in the second hydration shell of the calcium ion forming solvent-separated ion pairs. Ca–Cl contact ion pairs can be also found at 2.7–2.75 Å.

A new Cl–O^I contribution to the radial distribution function was also taken into account. The Cl–O^I was found to be around 3.8 Å when one or two water molecules are changed to chloride ions from the first hydration shell of the calcium ions.

On the basis of the coordination numbers obtained and the stoichiometric ratio for different concentrations we suggest several models that could well interpret our results. In low-concentration solution, the coordination number for the cation is eight and that for the anion is six. A distorted square antiprism structural unit was suggested by several authors^{10,11,18} for the cationic solvate shell (Figure 7a). The resulting coordination numbers and the Ca–O and O–O distances support this model. As it was already examined in previous works,^{4,50,51} the chemical type of the Cl–O interactions and the larger distances and σ values make the regular octahedral geometry for the anionic solvate less probable. In more concentrated solutions, the possible structural units could be six-coordinated calcium ion (Figure 7b) or contact ion pairs with one or two chloride ions connected to solvent molecules (Figure 7c,d).

TABLE 6: Structural Parameters for the CaCl_2 Solution in Methanol with the Estimated Errors in the Last Digits^a

sample	bond type	r	σ	n
1 M	Ca–O	2.39(1)	0.19	6.0
	Ca–O ^{II}	4.54(5)	0.22	11.2(9)
	Ca–Cl ^{II}	5.10	0.4	1.0
	O ^I –O ^I	3.40	0.20	4.0
	Ca–C	3.52(1)	0.20	6.0
	Cl–O	3.19(1)	0.20	6.0
	Cl–C	4.14(5)	0.22	6.0
	O–O	2.85(5)	0.20	1.7(4)
	C–O	3.61(1)	0.20	2.7(1)
	C–C	4.90(3)	0.23	5.5
2 M	Ca–O	2.39	0.19	5.1
	Ca–O ^{II}	4.55(5)	0.25	9.2(9)
	Ca–Cl	2.70(3)	0.18	1.1(1)
	O ^I –O ^I	3.50(1)	0.20	4.0
	Ca–C	3.67(1)	0.20	5.5
	Cl–O	3.22	0.20	6.0
	Cl–C	4.04(5)	0.23	6.0
	O–O	2.90(2)	0.20	1.1(1)
	C–O	3.64(2)	0.20	2.5(5)
	C–C	4.84(5)	0.25	5.0

^a The distances (r) and the mean square deviations (σ) are given in Å.

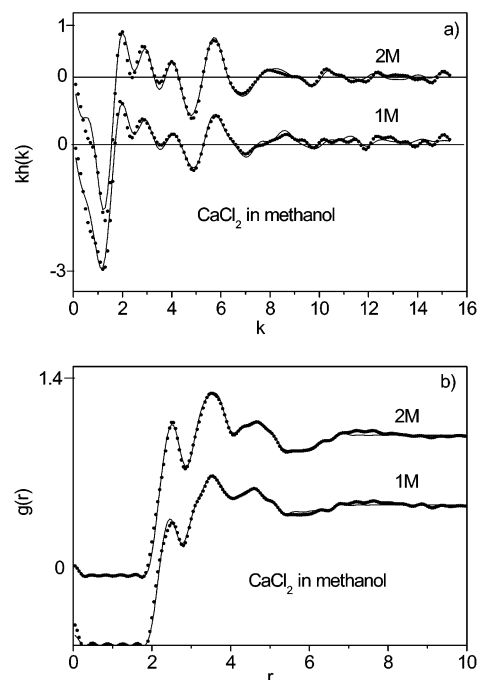


Figure 5. Structure functions, $h(k)$, multiplied by k (a) and pair correlation functions, $g(r)$ (b), for calcium chloride solution in methanol. The experimental values are given by dotted lines and the theoretical values by solid lines.

3.3.3. Methanol Solutions of CaCl_2 . In solutions of CaCl_2 in methanol, the stoichiometric ratio of Ca^{2+} ion to the number of methanol molecules equals 1:24.4 and 1:11.8 (Table 6). The structure functions for CaCl_2 solutions in methanol are shown in Figure 5a. For these solutions, it can be observed that the “double peak feature” described previously for aqueous solutions becomes less with increase in concentration, in other words, as the bulk of solvent is reduced by concentration.

The $g(r)$ functions are shown in Figure 5b. The Ca–O first-neighbor distances can be assigned to the first peak around 2.4 Å, which increases with concentration due to the increased weight of Ca–O-type contributions to the scattering pattern. A rather complex and broad main peak can be seen in the range

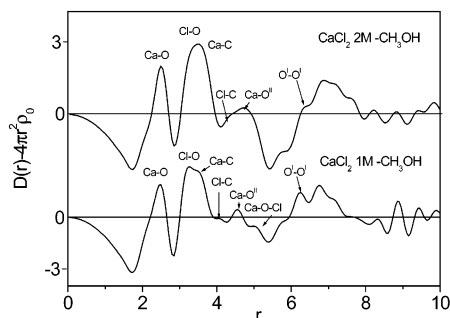


Figure 6. Difference radial distribution functions in the $D(r) - 4\pi r^2 \rho_0$ for each calcium chloride solution and pure methanol. The expected main contributions to the pair interactions are indicated by legends.

3–6 Å, which decomposes to two asymmetric peaks at about 3.55 Å, followed by a smaller peak at 4.6 Å.

X-ray Structure Functions and Radial Distribution Functions for CaCl_2 in Methanol. Figure 6 shows the difference radial distribution functions, $D(r) - 4\pi r^2 \rho_0$, for methanol solutions after subtraction of the corresponding distributions for pure methanol.^{46,52} Based on ionic radii listed above and the geometry of the methanol molecule,⁵² the characteristic distances of the most important contributions are denoted in the figures as legends. For the broad peak around 2–3 Å, mostly Ca–O interaction is responsible, but especially at higher concentration, it overlaps with minor contributions from the O–O (around 2.8 Å) and Ca–Cl (around 2.7 Å) type interactions. On the difference radial distribution function for the 2 M solution, the peak assigned to Ca–O interaction increases probably due to the appearance of Ca–Cl contact ion pairs in higher concentration solutions. The next peak around 3.6 Å can be assigned to Cl–O and Ca–C interactions. Further peaks are very difficult to analyze, because many different interactions appear at the same distance. For example, interaction due to Ca–O^{II} second solvation shell contributes to the peak at 4.6 Å, but also interactions between the oxygen atoms belonging to the solvation shell of calcium or chloride ions arise at this distance. The Ca–O–Cl solvent-separated ion pair is mostly responsible for the peak around 5.0 Å, and the peak at 6.4 Å arises from the interaction between the oxygen atoms in the solvation shell of a chloride ion. The peak assigned to the second solvation shell of the calcium ion becomes sharper with increase in concentration and that attributed to Ca–O–Cl solvent-separated ion pair disappears. Especially at higher concentrations, other interactions can contribute to peaks at such long distances, for example, the Ca–Cl–O (to the peak at 5.0 Å) and the long Ca–Cl–C (to the peak at 6.4 Å) interactions, namely, the interaction of a calcium ion from the Ca–Cl contact ion pair with an oxygen atom or a carbon atom from the solvation shell of a chloride ion.

Interpretation of the Structural Parameters and Model Building. Table 6 shows the structural parameters obtained from the least-squares fit of the structure functions for methanol solutions of CaCl_2 . The fitting procedure was described above.

The coordination number for the Ca^{2+} ion in 1 M solution resulted to be six. From the Ca–O, O–O^I (interaction of oxygen atoms involved in the coordination shell with oxygen atoms from bulk), and Ca–C distances, as well as the low mean square deviations, it can be concluded that the Ca–O solvation shell is octahedral. With increase in concentration, the Ca–O coordination number slightly decreases and the change in O–O^I and Ca–C parameters suggest that the octahedral coordination shell is destroyed. The O–O interaction can be observed around 2.85–2.9 Å even at high concentrations, suggesting that the

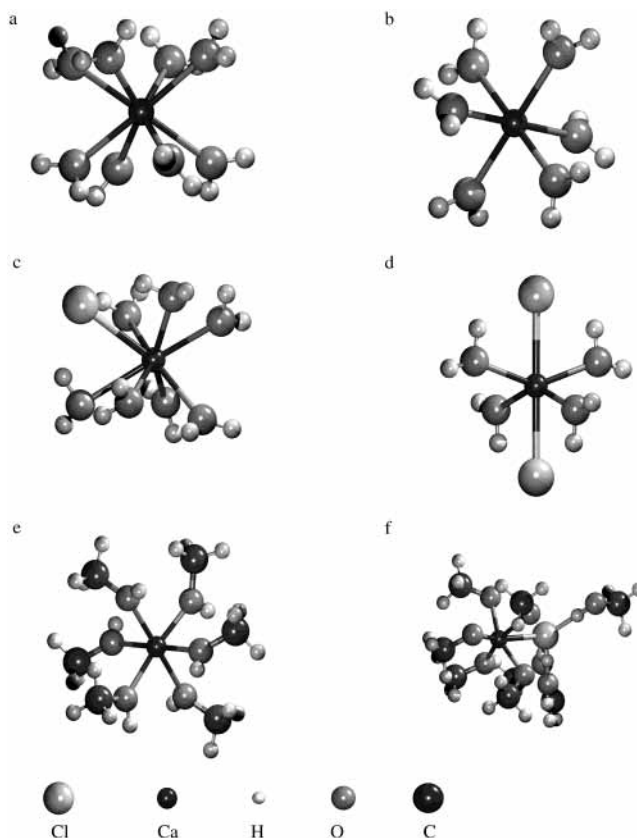


Figure 7. Ball and stick representation of possible models for aqueous and methanol solutions: (a) distorted square antiprism in aqueous solution; (b) octahedral solvation shell; (c) Ca–Cl contact ion pair in aqueous solution; (d) Cl–Ca–Cl contact ion pair in aqueous solution; (e) octahedral solvation shell in methanol; (f) Ca–Cl contact ion pair in methanol solution.

interaction among methanol molecules will not disappear completely. Taking into account the considerations above and the stoichiometry of the solutions, this is only possible if contact or solvent-separated ion pairs or both are formed and bulk methanol remains in the solution. In 1 M solution, the Ca–O–Cl solvent-separated ion pair distance is found to be around 5.1 Å and the coordination number is 1. Contact ion pairs have not been found in the 1 M solution, probably because they are not present and all ions are solvated, but it is true that even if they are present, their contribution to the structure function is very low at this concentration. In 2 M solution, solvent-separated ion pairs cannot be detected at 5.1 Å, but Ca–Cl contact ion pairs can be found around 2.75 Å. The second solvation shell of calcium ions appears at around 4.55 Å. The number of solvent molecules in the second solvation shell decreases with concentration from 11 to 9. In low-concentration solution, the Cl^- ion is solvated by six methanol molecules as it can be revealed from Cl–O and Cl–C parameters. Models suggested for methanol solutions are as follows. The calcium ion is six-coordinated; thus, its solvation shell has presumably octahedral symmetry as results from the Ca–O, O–O, and Ca–C distances and coordination numbers (Figure 7e). The coordination number for the chloride ion is also six, but as it was described above the regular octahedral geometry for the chloride ion is less probable. In 1 M solution, solvent-separated ion pairs can be found, while in 2 M solution, the octahedral solvation shell of the calcium ion is destroyed and Ca–Cl contact ion pairs are formed (Figure 7f); the solvation shells of the calcium and chloride ions are forced to share methanol molecules.

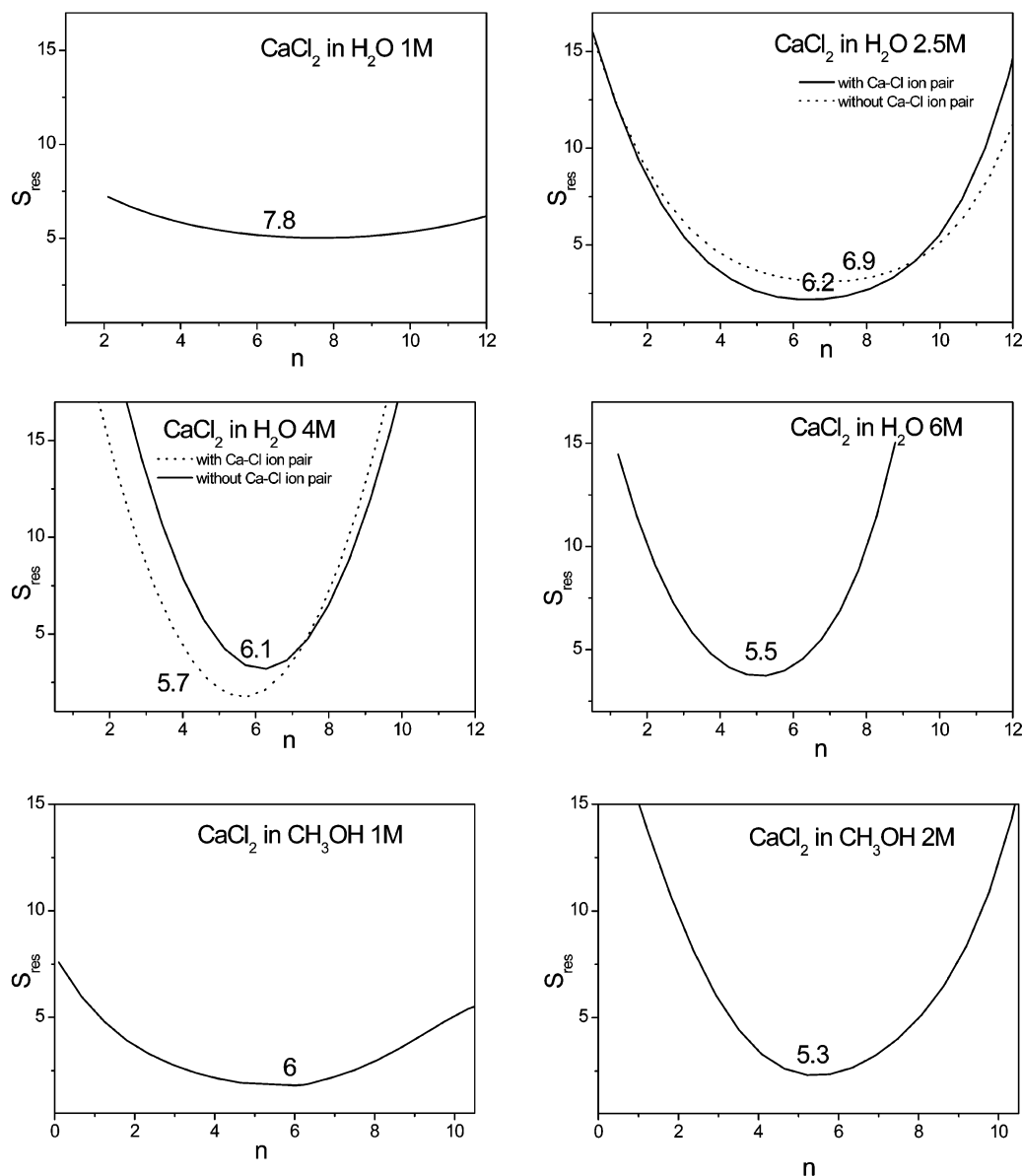


Figure 8. Variation of the error square sum (S_{res}), defined in eq 3, with the coordination number (n) of calcium ion in aqueous and methanol solutions. The value of the coordination number at minimum of the error square sum is marked on the figure.

3.3.4. Reliability of the Data Analysis. To perform a further check on the results obtained from X-ray measurements, an attempt was made for further refinement of the coordination numbers. Starting from the best fitting model, we have tried to “walk around” the minimum obtained during the least-squares fit of the structure functions. In this attempt, all structural parameters were fixed except one or two coordination numbers and the changes in the local minimum of the residual curve were calculated as a function of coordination numbers. The results are shown in Figure 8. It can be observed that for 1 M solutions both for water and methanol a broad, flat minimum is obtained due to the small contribution of the varied Ca–O contribution to the total structure function. The coordination number for the calcium ion in the minimum is 7.8 in aqueous solution and 6 in methanol. In addition, for 2.5 M aqueous solution, we have checked two models, one containing no contact ion pairs (M1) and another one assuming the presence of contact ion pairs in the solution (M2). The model containing contact ion pairs (M2) resulted only in a slightly better fit. The coordination number of calcium ion was found to be 6.9 for model M1 and 6.2 for model M2. For more concentrated

solutions, the coordination number decreased with increasing concentration and thus resulted in 5.7 and 5.5 for 4 and 6 M aqueous solutions, respectively. It can be concluded that in less concentrated solutions where the weights of the examined contributions are low, the determination of coordination number is rather uncertain and the results obtained for low-concentration solutions should be interpreted by taking into account the above considerations. In more concentrated solutions, the coordination numbers can be determined more precisely, but in these solutions, we have to take into account the possibility of ion pair formation.

4. Summary and Conclusions

Although the diffraction methods are known for the solution chemists as “direct methods for structural determination”, this means only that, in principle, the parameters obtainable from radial distributions are characteristic of local structures in the liquid directly and no further speculation is needed for extracting them from the experimental data. However, the solvate structure of calcium ion is a very good example when one can see that

even after decades of structural studies and gathering many structural data by many authors, some of the main questions are still open. The results presented here try to highlight some of the factors why this is so and try to answer some of the open questions.

One of the main questions is what is the reason for the large scatter in coordination numbers published for calcium ion? Does it really vary in a wide range or it is the accuracy of the determination too low to draw a definite conclusion? In the present work, we added four important conclusions to approach an answer.

(i) We have applied the available most accurate ab initio methods and determined the binding energies of each solvate molecule added, one by one, to the $\text{Ca}(\text{S})_n^{2+}$ complex, S being either water or methanol, and concluded that when n is large enough, the binding energies change only slightly and they reach a value when they can already compete with hydrogen-bonding energies between solvent molecules. This limit can be reached at number $n = 8$ for water and $n = 6$ for methanol; thus an essential point is taken with showing that the method is sensitive enough to reveal differences in the effect of solvent. Moreover, cross-checking of DFT and MP2 methods supports the idea that the calculations give realistic results. Consequently, we expect that the experimental solvation numbers may exhibit a large variation and this is due to the loose solvation around calcium ion. The speculation about octahedral or higher but still regular symmetry in the first coordination shell can also be concluded: while at six coordination the octahedral arrangement is obviously the most stable one, any attempt to place more molecules in the complex will break the symmetry. In contrast, the counterion, chloride, shows its usual stability: the coordination number is six even at high concentration but without the octahedral symmetry.

(ii) We have investigated a wide concentration series rather than individual experiments both on aqueous and on methanol solutions of calcium chloride. A concentration effect has been found: with increasing concentration, the coordination number of calcium decreased. Careful and extensive model building helped us to reveal the discussed four-step mechanism of turning the fully solvated ions to distorted solvation shells, then solvent-separated and finally contact ion pairs (still partially solvated). This mechanism well explains the decrease in coordination number with the lack of solvent molecules at high concentration but, on the other hand, again supports the idea that calcium ion is ready to lose its solvating molecules, thus rearranging the solvation structure; the chloride ion again remains six-coordinated even when the concentration is high.

(iii) This is the first case when a series of methanol solutions of calcium ion have been studied by X-ray diffraction. This helped us to compare the effect of solvent molecules on the structure, and indeed, the appearance of methyl group in the molecule and the consequent breaking up of the extended hydrogen-bonded structure in the bulk liquid led to significant differences in solvation by smaller coordination number for methanol than water and, in addition, the appearance of contact ion pairs instead of solvent-separated ones at relatively high concentration. Thus an additional conclusion is obvious: calcium solvation is sensitive to the sort of solvating molecule as well.

(iv) Finally, the sensitivity of the experimental method has been also a subject of tests. With the "constrained fit" method, we demonstrated that the X-ray diffraction method is not sensitive enough to decide the coordination number of calcium ion with high precision: in such a way, we face an unfortunate

coincidence of the uncertainty of the method and the inherent uncertainty due to the physical character of the ion in question. It is important to emphasize that while X-ray diffraction (and we may add that neutron diffraction is not at all better) fails in precise determination of coordination number, the method is performing very well in determination of Ca^{2+} -O distances: the obtained values fell in range 2.43–2.46 Å for aqueous solutions, well within the error limits, and in case of methanol solutions, they resulted in a slightly lower (2.39 Å) value but one well in the range of error limit as well, a feature which was also observed earlier, for other cations, for example, Mg^{2+} .

The authors should add another remark here. We are aware of the fact that all these conclusions can be considered true in the understanding that all applied methods will reflect only an averaged picture and the models used for fitting the data do not include the possibility of having several structures realized almost simultaneously. In other words, the methods are not able to reflect the effects of the fast dynamics, for example, at a time scale of NMR data, which show that the mean residence time of a water ligand in the first hydration shell of $\text{Ca}(\text{II})$ is between 10^{-9} and 10^{-11} seconds. Such fast dynamics can be associated with very rapid changes of coordination numbers and geometry of the solvate, which, once accessed, can lead to better understanding of the solvation of Ca^{2+} ion.

Acknowledgment. The research was supported by the Hungarian Scientific Research Funds (OTKA), Project Numbers T043676 and M36946. Imre Bakó is grateful to the Hungarian Academy of Sciences for supporting this work with a Bolyai stipend.

References and Notes

- Ohtaki, H.; Radnai, T. *Chem. Rev.* **1993**, *93*, 1157.
- Ohtaki, H. *Pure Appl. Chem.* **1987**, *59*, 1143.
- Johansson, G. *Adv. Inorg. Chem.* **1992**, *39*, 159.
- Probst, M. M.; Radnai, T.; Heinzinger, K.; Bopp, P.; Rode, B. M. *J. Phys. Chem.* **1985**, *89*, 753.
- Albright, J. N. *J. Chem. Phys.* **1972**, *56*, 3783.
- Smirnov, P.; Yamagami, M.; Wakita, H.; Yamaguchi, T. *J. Mol. Liq.* **1997**, *73–74*, 305.
- Licheri, G.; Piccaluga, G.; Pinna, G. *J. Chem. Phys.* **1976**, *64*, 2437.
- Cummings, S.; Enderby, J. E.; Howe, R. A. *J. Phys. C* **1980**, *13*, 1.
- Hewish, N. A.; Neilson, G. W.; Enderby, J. E. *Nature* **1982**, *297*, 138.
- Spangberg, D.; Hermansson, K.; Lindqvist-Reis, P.; Jalilehvand, F.; Sandström, M.; Persson, I. *J. Phys. Chem. B* **2000**, *104*, 10467.
- Jalilehvand, F.; Spangberg, D.; Lindqvist-Reis, P.; Hermansson, K.; Persson, I.; Sandström, M. *J. Am. Chem. Soc.* **2001**, *123*, 431.
- Fulton, J. L.; Heald M. S.; Badyal, Y. S.; Simonsom, J. M. *J. Phys. Chem. A* **2003**, *107*, 4688.
- Pálinkás, G.; Heinzinger, K. *Chem. Phys. Lett.* **1986**, *126*, 251.
- Floris, F. M.; Persico, M.; Tani, A.; Thomasi, J. *Chem. Phys. Lett.* **1994**, *227*, 126.
- Bernal-Uruchurtu, M. I.; Ortega-Blake, I. *J. Chem. Phys.* **1995**, *103*, 1588.
- Kalko S. G.; Sesé, G.; Padro, J. A. *J. Chem. Phys.* **1996**, *104*, 9578.
- Obst, S.; Bradaczek, H. *J. Phys. Chem.* **1996**, *100*, 15677.
- Tongraar, A.; Liedl, K. R.; Rode, B. M. *J. Phys. Chem. A* **1997**, *101*, 6299.
- Pavlov, M.; Siegbahn, E. M.; Sandström, M. *J. Phys. Chem. A* **1998**, *102*, 219.
- Schwenk, C. F.; Loeffler, H. H.; Rode, B. M. *J. Chem. Phys.* **2001**, *115*, 10808.
- Katz Kaufmann, A.; Glusker, J. P.; Beebe, S. A.; Bock, C. W. *J. Am. Chem. Soc.* **1996**, *118*, 5752.
- Bakó, I.; Hutter, J.; Pálinkás, G. *J. Chem. Phys.* **2002**, *117*, 9838.
- Naor, M. M.; Nostrand, V. K.; Dellago, C. *Chem. Phys. Lett.* **2003**, *369*, 159.
- Kahlow, M. A.; Jarzeba, W.; Kang, T. J.; Barbara, P. F. *J. Chem. Phys.* **1989**, *90*, 151.
- Roy, S.; Bagchi, B. *J. Chem. Phys.* **1994**, *101*, 4150.
- Wahab, A.; Mahiuddin, S. *J. Chem. Eng. Data* **2001**, *46*, 1457.
- Kim, H. S. *J. Mol. Struct. (THEOCHEM)* **2001**, *541*, 59.

- (28) (a) Becke, A. D. *Phys. Rev. A* **1988**, *38*, 3098. (b) Lee, C.; Yang, W.; Parr, R. C. *Phys. Rev. B* **1988**, *37*, 785.
- (29) Frisch, M. J.; Trucks, G. W.; Schlegel, H. B.; Scuseria, G. E.; Robb, M. A.; Cheeseman, J. R.; Zakrzewski, V. G.; Montgomery, J. A., Jr.; Stratmann, R. E.; Burant, J. C.; Dapprich, S.; Millam, J. M.; Daniels, A. D.; Kudin, K. N.; Strain, M. C.; Farkas, O.; Tomasi, J.; Barone, V.; Cossi, M.; Cammi, R.; Mennucci, B.; Pomelli, C.; Adamo, C.; Clifford, S.; Ochterski, J.; Petersson, G. A.; Ayala, P. Y.; Cui, Q.; Morokuma, K.; Malick, D. K.; Rabuck, A. D.; Raghavachari, K.; Foresman, J. B.; Cioslowski, J.; Ortiz, J. V.; Stefanov, B. B.; Liu, G.; Liashenko, A.; Piskorz, P.; Komaromi, I.; Gomperts, R.; Martin, R. L.; Fox, D. J.; Keith, T.; Al-Laham, M. A.; Peng, C. Y.; Nanayakkara, A.; Gonzalez, C.; Challacombe, M.; Gill, P. M. W.; Johnson, B. G.; Chen, W.; Wong, M. W.; Andres, J. L.; Head-Gordon, M.; Replogle, E. S.; Pople, J. A. *Gaussian 98*, revision A.7; Gaussian, Inc.: Pittsburgh, PA, 1998.
- (30) Peschke, M.; Blades, A. T.; Kebarle, P. *Int. J. Mass Spectrom.* **1999**, *185–187*, 685.
- (31) Boys, S.; Bernardi, F. *Mol. Phys.* **1970**, *19*, 553.
- (32) Glendening, E. D.; Feller, D. *J. Phys. Chem.* **1996**, *100*, 4790.
- (33) Lindgren, J.; Hermanson, K.; Wojcik, M. *J. Phys. Chem.* **1993**, *97*, 5254.
- (34) Garcia-Muruais, A.; Cabaleiro-Lago, E. M.; Hermida-Ramon, J. M.; Rios, M. A. *Chem. Phys.* **2000**, *254*, 109.
- (35) (a) Borell, M. M.; Leclaire, A. *Acta Crystallogr.* **1977**, *B33*, 2940. (b) Fruchart, P. D.; Backmann, M.; Chaudouet, P. *Acta Crystallogr.* **1980**, *B36*, 2759.
- (36) Radnai, T.; Ohtaki, H. *Mol. Phys.* **1996**, *87*, 103.
- (37) Hajdu, F.; Pálinkás, G. *J. Appl. Crystallogr.* **1972**, *5*, 395.
- (38) Levy, H. A.; Danford, M. D.; Narten, A. H. *Oak Ridge National Laboratory Report*; Report No. 3960; Oak Ridge National Laboratory: Oak Ridge, TN, 1966.
- (39) Hajdu, F. *Acta Crystallogr.* **1972**, *A28*, 250.
- (40) Pálinkás, G.; Radnai, T. *Acta Crystallogr.* **1976**, *A32*, 666.
- (41) Krogh-Moe, K. *J. Acta Crystallogr.* **1956**, *2*, 951.
- (42) Cromer, D. T.; Waber, J. T. *Acta Crystallogr.* **1965**, *A32*, 104.
- (43) *International Tables for X-ray Crystallography*; The Kynoch Press: Birmingham, AL, 1974; Vol 4.
- (44) Levy, H. A.; Danford, M. D.; Narten, A. H. *Oak Ridge National Laboratory Report*; Report No. 3960; Oak Ridge National Laboratory, Oak Ridge, TN, 1966.
- (45) Reichardt, C. *Solvents and Solvent Effects in Organic Chemistry*, 2nd ed.; VCH: Weinheim, Germany, 1988. Marcus, Y. *Ion Solvation*; Wiley: Chichester, U.K., 1985.
- (46) Narten, A. H. *J. Chem. Phys.* **1971**, *55*, 2263.
- (47) Megyes, T.; Grósz, T.; Radnai, T.; Pálinkás, G. Unpublished data measured in X-ray Laboratory, Chemical Research Centre, Hungarian Academy of Sciences.
- (48) Náráy Szabó, I. *Kristálykémiá*; Akadémiai Kiadó: Budapest, Hungary, 1965; p 60.
- (49) Yamaguchi, T.; Hayashi, S.; Ohtaki, H. *Inorg. Chem.* **1989**, *28*, 2434.
- (50) Radnai, T.; Bakó, I.; Pálinkás, G. *ACH—Models Chem.* **1995**, *132*, 159.
- (51) Tongraar, A.; Rode, B. M. *Phys. Chem. Chem. Phys.* **2003**, *5*, 357.
- (52) Narten, A. H.; Habenschuss, A. *J. Chem. Phys.* **1984**, *80*, 3387.